Published in final edited form as:
Nature. 2014 April 10; 508(7495): 258–262. doi:10.1038/nature13198.

Nicotinamide *N*-methyltransferase knockdown protects against diet-induced obesity

Daniel Kraus[1,†,*], **Qin Yang**[1,*,†], **Dong Kong**[1], **Alexander S. Banks**[2], **Lin Zhang**[1], **Joseph T. Rodgers**[2], **Eija Pirinen**[3,†], **Thomas C. Pulinilkunnil**[1,†], **Fengying Gong**[1,†], **Ya-chin Wang**[1], **Yana Cen**[4], **Anthony A. Sauve**[4], **John M. Asara**[5], **Odile D. Peroni**[1], **Brett P. Monia**[6], **Sanjay Bhanot**[6], **Leena Alhonen**[3,†], **Pere Puigserver**[2], and **Barbara B. Kahn**[1]

[1]Division of Endocrinology, Diabetes, and Metabolism, Department of Medicine, Beth Israel Deaconess Medical Center and Harvard Medical School, 330 Brookline Avenue, Boston, Massachusetts 02215, USA [2]Department of Cancer Biology, Dana-Farber Cancer Institute, Harvard Medical School, Boston, Massachusetts 02115, USA [3]Biotechnology and Molecular Medicine, A.I. Virtanen Institute for Molecular Sciences, Biocenter Kuopio, University of Eastern Finland, Kuopio Campus, PO Box 1627, FI-70211 Kuopio, Finland [4]Department of Pharmacology, Weill Medical College of Cornell University, 1300 York Avenue, New York, New York 10065, USA [5]Division of Signal Transduction, Beth Israel Deaconess Medical Center and Harvard Medical School, 330 Brookline Ave, Boston, Massachusetts 02215, USA [6]Isis Pharmaceuticals, 1896 Rutherford Road, Carlsbad, California 92008-7326, USA

Abstract

†Present addresses: Division of Nephrology, Department of Internal Medicine I, Würzburg University Hospital, Oberdürrbacher Straße 6, 97080 Würzburg, Germany (D.K.); Department of Medicine, Physiology and Biophysics, Center for Diabetes Research and Treatment, and Center for Epigenetics and Metabolism, University of California, Irvine, California 92697, USA (Q.Y.); Research Programs Unit, Molecular Neurology, Biomedicum Helsinki, University of Helsinki, 00290, Helsinki, Finland (E.P.); Department of Biochemistry and Molecular Biology, Faculty of Medicine, Dalhousie Medicine New Brunswick, Dalhousie University, Saint John, New Brunswick E2L4L5, USA (T.C.P.); Department of Endocrinology, Key Laboratory of Endocrinology of Ministry of Health, Peking Union Medical College Hospital, Chinese Academy of Medical Sciences and Peking Union Medical College, Beijing 100730, China (F.G.); School of Pharmacy, University of Eastern Finland, P.O. Box 1627, FI-70211 Kuopio, Finland (L.A.).
*These authors contributed equally to this work.

Online Content

Any additional Methods, Extended Data display items and Source Data are available in the online version of the paper; references unique to these sections appear only in the online paper.

Supplementary Information is available in the online version of the paper.

Author Contributions

Q.Y. discovered NNMT from the initial microarray analysis. D.Kr., Q.Y. and B.B.K designed the experiments, interpreted the data and wrote the paper. D.Ko. performed oxygen consumption experiments in adipocytes. A.S.B. performed CLAMS studies. L.Z., T.C.P., F.G., YC.W. and O.D.P. provided assistance with cell culture and animal experiments. O.D.P. also performed the microarray studies. J.T.R. and P.P. performed PGC-1α acetylation experiments. E.P. and L.A. provided expertise on polyamines and measured ODC and SSAT activity. Y.C. and A.A.S. measured nicotinamide and metabolites. J.M.A. performed metabolomics studies. B.P.M and S.B. provided *Nnmt* and control ASOs.

Author Information

The microarray data from adipose tissue of adipose-specific knockout and adipose-specific overexpression have been published by our laboratory and are available in NCBI Gene Expression Omnibus under accession number GSE35378. Reprints and permissions information is available at www.nature.com/reprints. The authors declare competing financial interests: details are available in the online version of the paper. Readers are welcome to comment on the online version of the paper. Correspondence and requests for materials should be addressed to B.B.K. (bkahn@bidmc.harvard.edu) or Q.Y. (qin.yang@uci.edu).

In obesity and type 2 diabetes, *Glut4* glucose transporter expression is decreased selectively in adipocytes[1]. Adipose-specific knockout or overexpression of *Glut4* alters systemic insulin sensitivity[2]. Here we show, using DNA array analyses, that nicotinamide *N*-methyltransferase (*Nnmt*) is the most strongly reciprocally regulated gene when comparing gene expression in white adipose tissue (WAT) from adipose-specific *Glut4*-knockout or adipose-specific *Glut4*-overexpressing mice with their respective controls. NNMT methylates nicotinamide (vitamin B3) using *S*-adenosylmethionine (SAM) as a methyl donor[3,4]. Nicotinamide is a precursor of NAD^+, an important cofactor linking cellular redox states with energy metabolism[5]. SAM provides propylamine for polyamine biosynthesis and donates a methyl group for histone methylation[6]. Polyamine flux including synthesis, catabolism and excretion, is controlled by the rate-limiting enzymes ornithine decarboxylase (ODC) and spermidine–spermine N^1-acetyltransferase (SSAT; encoded by *Sat1*) and by polyamine oxidase (PAO), and has a major role in energy metabolism[7,8]. We report that NNMT expression is increased in WAT and liver of obese and diabetic mice. *Nnmt* knockdown in WAT and liver protects against diet-induced obesity by augmenting cellular energy expenditure. NNMT inhibition increases adipose SAM and NAD^+ levels and upregulates ODC and SSAT activity as well as expression, owing to the effects of NNMT on histone H3 lysine 4 methylation in adipose tissue. Direct evidence for increased polyamine flux resulting from NNMT inhibition includes elevated urinary excretion and adipocyte secretion of diacetylspermine, a product of polyamine metabolism. NNMT inhibition in adipocytes increases oxygen consumption in an ODC-, SSAT- and PAO-dependent manner. Thus, NNMT is a novel regulator of histone methylation, polyamine flux and NAD^+-dependent SIRT1 signalling, and is a unique and attractive target for treating obesity and type 2 diabetes.

Nnmt is expressed at high levels in adipose tissue and liver and at lower levels in other organs[3,4]. *Nnmt* is increased in multiple cancers[9,10], neuro-degenerative diseases[11], and also in obesity and diabetes[12–14]. For example, *Nnmt* expression is increased in adipocytes of obese, compared to non-obese Pima Indians[12]. Metabolomic analyses reveal elevated levels of urinary N^1-methylnicotinamide, the product of NNMT, in humans with type 2 diabetes, and in *db*/*db* mice and obese Zucker rats[13], indicating increased NNMT activity in obesity and type 2 diabetes. Quantitative trait loci mapping in mice suggests a causative role of *Nnmt* in type 2 diabetes[14]. Therefore, we investigated the regulation and roles of NNMT in obesity and type 2 diabetes.

Adipose *Nnmt* messenger RNA levels were increased twofold in insulin-resistant adipose-specific *Glut4*-knockout mice (Fig. 1a), and reduced by 62% in insulin-sensitive adipose-specific *Glut4*-overexpressing mice (Fig. 1b). NNMT protein was increased 1.5- to 2-fold in WAT of *ob*/*ob*, *db*/*db* mice and high-fat diet (HFD)-fed mice (Fig. 1c–e), compared with lean, insulin-sensitive controls. Hepatic NNMT protein levels were increased in *ob*/*ob* and *db*/*db* mice (Fig. 1f, g) and tended to be higher in HFD-fed mice (Fig. 1h). Thus, NNMT is upregulated in adipose tissue and liver of mouse models of obesity and insulin resistance.

Adipose and hepatic *Nnmt* expression varies highly among 25 different mouse strains[15] (Supplementary Fig. 1). Adipose *Nnmt* expression is high in obesity-prone strains and low in obesity-resistant strains[15–17] (Supplementary Fig. 1a). In contrast, liver *Nnmt* expression does not parallel the propensity for obesity (Supplementary Fig. 1b). Adipose *Nnmt*

expression correlates highly with per cent fat mass in diet-induced obesity across 20 different mouse strains[18], and with expression of retinol-binding protein 4 (*Rbp4*) (r =0.90, P <0.0001 by Pearson correlation coefficient, two-tailed test), an adipokine that contributes to insulin resistance[2] (Supplementary Fig. 2a, b). Thus, we proposed that elevated NNMT levels in adipose tissue and/or liver may have a causative role in insulin resistance and obesity.

We knocked down *Nnmt* with antisense oligonucleotides (ASOs) in HFD-fed mice. ASOs regulate gene expression primarily in liver and fat[19,20]. Treating HFD-fed mice with *Nnmt* ASO reduced *Nnmt* mRNA and NNMT protein by 60 to 75% in WAT and 60% (protein) to 90% (mRNA) in liver (Fig. 2a–d), but not in brown adipose tissue and kidney (Fig. 2e, f). Serum transaminases and creatinine were normal, indicating no hepaticor renal toxicity with ASO treatment (Supplementary Fig. 3a–c).

Nnmt knockdown in adipose tissue and liver protected mice from diet-induced obesity (Fig. 2g), causing a 47% reduction in relative fat mass and a 15% increase in relative lean mass (Fig. 2h, i). Free body water and hepatic glycogen content were not different (not shown) between control- and *Nnmt*-ASO-treated mice. Subcutaneous and epididymal fat-pad weights were lower in *Nnmt*-knockdown mice than in controls (Fig. 2j, k), largely owing to reduced adipocyte size (44% reduced area, Fig. 2l, and 70% reduced volume, Supplementary Fig. 4). Insulin sensitivity was enhanced, as evidenced by approximately 50 to 60% lower serum insulin levels and glucose-insulin product (Fig. 2m, n). *Nnmt* knockdown also improved glucose tolerance (Fig. 2o, p), prevented HFD-induced hepatic steatosis(Fig. 2q, r), and decreased serum triglycerides and free fatty acids (Supplementary Fig. 5a, b). Thus, *Nnmt* knockdown in WAT and liver protects against diet-induced obesity and its deleterious metabolic consequences.

We sought to determine whether the leanness with *Nnmt* knockdown is due to reduced energy intake or increased energy expenditure. The NNMT substrate, nicotinamide, at pharmacological doses may suppress food intake and cause weight loss in rats[21]. However, *Nnmt*-ASO-treated mice consumed the same amount of calories as controls (Fig. 3a). Food intake was measured before body weights diverged, in order to eliminate confounding by body-weight differences. Feed efficiency (body weight change per kcal of food eaten) was reduced by approximately 50% in *Nnmt*-knockdown mice (Fig. 3b). Although control-ASO-treated mice gained about 7 mg of fat per kcal of food intake, *Nnmt*-ASO-treated mice gained no fat (Fig. 3c). Thus, body weight and fat gain were disproportionally low for the calorie intake in *Nnmt*-ASO-treated compared with control-ASO-treated mice. Faecal lipid excretion was not changed between control- and *Nnmt*-ASO-treated mice (Fig. 3d). Therefore, increased energy expenditure rather than decreased food intake or steatorrhoea explains the leanness in *Nnmt*-knockdown mice. This was further demonstrated by increased oxygen consumption (expressed per kg body weight or per mouse) during comprehensive laboratory animal monitoring system (CLAMS) analysis performed before body weights started to diverge (Fig. 3e and Supplementary Fig. 6a). Comparison of mice with similar body weight showed that *Nnmt*-ASO-treated mice had higher energy expenditure than control-ASO-treated mice (Supplementary Fig. 6b). Energy expenditure per gram of fat mass, but not per gram of lean mass was increased in *Nnmt*-ASO-treated mice compared

with control-ASO-treated mice (Supplementary Fig. 6c, d). There was no measurable difference in food intake expressed per mouse or per g body weight, locomotor activity or respiratory exchange ratio (RER) (Supplementary Fig. 7a–d). As a third approach to assess the energy expenditure, we measured body weight and body composition before and after an overnight fast. In the absence of energy intake, increased loss of body fat indicates increased energy expenditure. After fasting, *Nnmt*-knockdown mice on HFD lost more body weight, body fat and lean mass than control-ASO-treated mice, and the response resembled that of chow-fed lean mice (Fig. 3f–h). Core body temperature, BAT weight, and uncoupling protein-1 levels in BAT (Supplementary Fig. 8a–c) were unchanged. Thus, *Nnmt* knockdown in WAT and liver increases energy expenditure, and this is likely to be independent of BAT-induced energy dissipation or heat production.

We asked whether NNMT regulates energy expenditure in a cell-autonomous manner. *Nnmt* knockdown in adipocytes led to a 60% increase in oxygen consumption (Fig. 3i). NNMT inhibition by N^1-methylnicotinamide—the NNMT reaction product and a specific, potent inhibitor of NNMT at pharmacological doses[3]—also increased oxygen consumption (Fig. 3j). Conversely, *Nnmt* overexpression decreased oxygen consumption (Fig. 3k) in adipocytes. Similar results were obtained in cultured hepatoma cells (Supplementary Fig. 9). Therefore, NNMT regulates oxygen consumption in a cell-autonomous fashion in both adipocytes and hepatocytes.

We sought to determine the molecular mechanisms for increased energy expenditure with NNMT inhibition. NNMT methylates nicotinamide using SAM as a methyl donor and generates *S*-adenosylhomocysteine (SAH). Adipose SAM, and the SAM:SAH ratio were increased by 50% in *Nnmt*-ASO-treated mice (Fig. 4a). In liver, SAM was not changed, but the SAM:SAH ratio was increased by 2.2-fold owing to a 48% reduction of SAH levels in *Nnmt*-ASO-treated mice (Supplementary Fig. 10). The unchanged hepatic SAM with *Nnmt* knockdown contrasts with knockdown of glycine *N*-methyltransferase (*Gnmt*), a dominant methyltransferase that accounts for >1% of total cytosolic protein in liver. *Gnmt* knockdown increases SAM by 40-fold and induces hepatic steatosis and fibrosis[22]. Hepatic *Nnmt* knockdown did not cause fibrosis as evidenced by normal expression of tissue inhibitor of metal-loproteinase 1 (*Timp1*) and collagen type 1 (*Colla1*), markers for hepatic fibrosis (Supplementary Fig. 11a, b).

SAM has two major functions: first, providing propylamine groups for polyamine biosynthesis; and second, donating methyl groups to substrates including histones[6]. Polyamines (putrescine, spermine and spermidine) are organic polycations that are essential for multiple cellular functions affecting cell growth, cancer and ageing[23]. Polyamine metabolism is tightly controlled (Supplementary Fig. 12)[23]. Synthesis is controlled by ODC producing putrescine, and by adenosylmethionine decarboxylase (AMD1) providing decarboxylated SAM for the synthesis of spermidine and spermine. Catabolism is controlled by spermidine–spermine N^1-acetyltransferase (SSAT), which acetylates spermidine and spermine using acetyl-CoA as a substrate. The acetylated products including N^1-acetylspermine, N^1, N^{12}-diacetylspermine, and N^1-acetylspermidine, are either oxidized by PAO or excreted intact in urine. Polyamine flux has a major role in energy homeostasis. Genetic knockout of SSAT results in increased diet-induced obesity and transgenic SSAT

overexpression causes leanness owing to altered energy expenditure[7,8,24]. As *Nnmt* knockdown increases adipose SAM levels (Fig. 4a), we reasoned that this may cause a 'substrate shunt' of SAM from the NNMT reaction to polyamine flux leading to increased energy expenditure in *Nnmt*-ASO-treated mice (Fig. 3). In support of this, *Nnmt* expression correlates negatively with *Odc* and *Ssat* expression in adipose tissue, but not in liver in 25 different mouse strains[15] (Supplementary Fig. 13a–d).

Nnmt-ASO treatment *in vivo* augmented adipose ODC and SSAT activity (Fig. 4b, c) and mRNA expression (Fig. 4d). The expression of adenosylmethionine decarboxylase *Amd1*, which provides decarboxylated SAM for spermidine and spermine synthesis, was also increased (Fig. 4d). In liver, *Nnmt* ASO increased ODC, but not SSAT activity, or *Odc* or *Ssat* expression (Supplementary Fig. 14a–d). ODC and SSAT activation drives polyamine flux, which consumes the metabolic substrate, acetyl-CoA, for polyamine acetylation[7]. Consistent with reduced acetyl-CoA availability for lipogenesis, acetyl-CoA carboxylase 1 expression and fatty acid synthase expression and activity were decreased in adipose tissue of *Nnmt*-ASO-treated mice (Supplementary Fig. 15a–c). In addition, adipose *Nnmt* knockdown also decreased ATP, increased the AMP:ATP ratio and enhanced AMPK threonine 172 phosphorylation (Supplementary Fig. 16a–d). Increased urinary diacetylspermine provides direct evidence for enhanced adipose polyamine flux in *Nnmt*-ASO-treated mice (Fig. 4e). Furthermore, reduction in *Nnmt* increased *Odc* and *Ssat* expression in cultured adipocytes (Fig. 4f, g). N^1-methylnicotinamide treatment promoted diacetylspermine secretion from adipocytes in a dose-dependent manner (Fig. 4h), complementing the increased urinary diacetylspermine excretion in *Nnmt*-ASO-treated mice (Fig. 4e). These data convincingly show that NNMT directly regulates polyamine flux in adipocytes.

In addition to being a substrate for polyamine metabolism, SAM is a methyl donor for numerous methylation reactions including histone methylation, which is important for transcriptional regulation[6]. We measured eight types of histone methylation; the amounts of mono-, di- or tri-methylated lysine 4 of histone H3 (H3K4) were increased in adipose tissue of *Nnmt*-ASO-treated mice (Fig. 4i). Chromatin immunoprecipitation followed by quantitative PCR (ChIP–qPCR) revealed enrichment of methylated H3K4 on *Odc* and *Ssat* genes with NNMT inhibition in adipocytes (Fig. 4j). Thus, NNMT inhibition modifies histone methylation and increases *Odc* and *Ssat* expression, leading to activation of polyamine flux.

To determine whether the increased energy expenditure with NNMT inhibition (Fig. 3) is polyamine-dependent, we used N^1-methylnicotinamide to inhibit NNMT activity in adipocytes. This induced oxygen consumption (Fig. 4k–m). Knocking down *Ssat* (Supplementary Fig. 17), inhibiting ODC activity[8] or blocking PAO activity abolished N^1-methylnicotinamide-induced oxygen consumption (Fig. 4k–m). Thus, NNMT inhibition in adipocytes autonomously enhances oxygen consumption, and this depends on polyamine flux.

The other substrate of the NNMT reaction is nicotinamide, an NAD^+ precursor. *Nnmt* ASO treatment did not alter adipose and hepatic nicotinamide levels (Supplementary Fig. 18a, b).

This is likely to be because nicotinamide is metabolized to NAD^+ in a salvage pathway, which is controlled by the rate-limiting enzymes nicotinamide phosphoribosyl-transferase (NAMPT) and three isoforms of nicotinamide mononucleotide adenylyltransferase (NMNAT1, NMNAT2 and NMNAT3)[5]. *Nnmt* knockdown increased NAD^+ levels per mg of adipose tissue (Fig. 4n) and the expression of *Nampt* (Fig. 4o), cytosolic *Nmnat2* and mitochondrial *Nmnat3*, but not nuclear *Nmnat1* (Supplementary Fig. 19). NAD^+ is a cofactor of SIRT1 deacetylase activity, and SIRT1 affects energy metabolism[5]. Expression of SIRT1 target genes, including *Cd36*, catalase (*Cat*), succinate dehydrogenase B (*Sdhb*) and growth-arrest and DNA-damage-inducible protein, were increased in adipose tissue of *Nnmt*-ASO-treated mice[25–28] (Fig. 4p), consistent with SIRT1 activation. As *Nnmt*-ASO-treated mice are leaner, NAD^+ levels per adipocyte may not be as elevated as per mg of adipose tissue. However, the increased gene expression upstream and downstream of NAD^+ strongly supports enhanced NAD^+ flux in *Nnmt*-ASO-treated adipocytes. In liver, *Nnmt* knockdown did not alter NAD^+ levels or the expression of *Nampt*, *Nmnat1*, *Nmnat2* or *Nmnat3* (Supplementary Fig. 20a, b). In spite of this, *Cd36, Cat and SdhB* expression was decreased (Supplementary Fig. 20c), indicating reduced SIRT1 activity. Consistent with this, PGC-1α acetylation was enhanced in liver with *Nnmt* knockdown[29] (Supplementary Fig. 20d). The decreased hepatic *Sirt1* expression (Supplementary Fig. 20e) may contribute to the reduced SIRT1 activity with *Nnmt* knockdown. Despite the changes in SIRT1 and PGC-1α activity, hepatic *Pck1* and *G6pc* expression were not altered by *Nnmt* ASO treatment (Supplementary Fig. 21).

We discovered that NNMT is a novel regulator of adiposity and energy expenditure. This involves modulating adipose SAM and NAD^+, two fundamental metabolites for energy metabolism. NNMT also regulates hepatic energy metabolism (Supplementary Fig. 9), but most likely with different mechanisms, as *Nnmt* knockdown did not alter hepatic SAM and NAD^+ levels. In adipocytes, SAM provides substrate for polyamine synthesis, and also modulates *Odc* and *Ssat* expression by modifying H3K4 methylation (Fig. 4q). SAM availability may alter histone methylation in a methylation-site-specific manner rather than affecting global histone methylation[10]. For example, threonine-regulated SAM specifically affects H3K4me3 in mouse embryonic stem cells[30]. NNMT-regulated H3K4 methylation may have broader effects on gene expression including effects associated with cancer[10] and dementia, conditions in which NNMT activity is enhanced[10,11].

Activation of adipose polyamine flux causes leanness by catalysing polyamine acetylation to generate acetylpolyamines using acetyl-coA as a metabolic substrate[7]. Acetylpolyamines are oxidized in a futile cycle or excreted in the urine, thereby reducing acetyl-CoA in cells (Fig. 4q and Supplementary Fig. 12). Although urinary excretion of acetyl-polyamines may not cause significant total-body calorie loss, the metabolic substrate consumption or loss in adipocytes seems to impact systemic energy expenditure. This is clearly demonstrated by leanness and increased energy expenditure in adipose *Ssat* transgenic mice[24]. Promoting consumption or loss of adipose acetyl-CoA as a metabolic substrate in the form of acetylpolyamines may be a novel strategy for obesity treatment (Fig. 4q).

NNMT regulates SAM and NAD^+ primarily in adipose tissue, but not in liver, which has redundant regulatory pathways for SAM and NAD^+ metabolism. Hepatic SAM is largely

regulated by glycine *N*-methyltransferase[22] and by methionine, an abundant SAM precursor in liver. When methionine is abundant, NNMT regulates only SAH, not SAM[10]. Liver NAD^+ synthesis is controlled by a salvage pathway using nicotinamide as a precursor and a *de novo* pathway using tryptophan[5]. In contrast, adipose tissue barely expresses the key enzymes in the *de novo* NAD^+ synthesis pathway (data not shown). Therefore, adipose NAD^+ synthesis primarily relies on the salvage pathway using nicotinamide, for which NNMT is the only catabolic enzyme. The adipose-selective effects of NNMT inhibition on SAM and NAD^+ levels are advantageous for drug development because increased SAM in liver causes hepatic steatosis and fibrosis[22], and increased NAD^+ may enhance hepatic gluconeogenesis[29].

In summary, NNMT is a unique regulator of adiposity by directly altering NAD^+ and SAM, which affect histone methylation, polyamine flux and SIRT1 signalling. NNMT inhibition leads to metabolic substrate consumption or loss from adipocytes coupled with increased energy expenditure in a cell-autonomous manner (Fig. 4q). These unique features render NNMT an attractive target for treating obesity and type 2 diabetes.

METHODS

Mice

Adipose-specific *Glut4*-knockout and *Glut4*-overexpressing mice were described previously[31,32]. All other mice were purchased from Jackson Laboratories or Charles River Laboratories. For measurements of *Nnmt* expression in adipose tissue and liver, the *ob*/*ob* and *db*/*db* mice were killed at 10 to 12 weeks of age. High-fat diet (HFD)-fed male mice in C57BL/6 background were treated with a HFD for 12 weeks starting at 6 to 8 weeks of age. For *Nnmt* ASO experiments, mice were fed standard chow providing 17% calories from fat (LabDiet Formulab 5008) or a HFD providing 55% calories from fat (Harlan Teklad, TD93075) starting at 6 to 7 weeks of age. *Nnmt* and control ASOs were injected at a dose of 37.5 mg kg^{-1} intraperitoneally twice per week starting 2 weeks after the initiation of HFD feeding. Mouse studies were conducted in accordance with federal guidelines and were approved by the Beth Israel Deaconess Medical Centre (BIDMC) Institutional Animal Care and Use Committee.

Selection of mouse *Nnmt* ASO

Rapid-throughput screens were performed in primary hepatocytes to identify mouse *Nnmt* antisense oligonucleotides. In brief, 80 ASOs were designed to the *Nnmt* mRNA sequence and tested in primary hepatocytes to identify *Nnmt* antisense oligonucleotides. *Nnmt* gene knockdown was screened by quantitative PCR. Eight ASOs were selected and further characterized in a dose–response screen *in vivo*. Two *Nnmt* ASOs with greatest effects on *Nnmt* knockdown in liver and adipose tissue with no toxicity to liver and kidney were used to treat mice on a HFD. Treatment with either of the *Nnmt* ASOs resulted in leanness compared with a control-ASO-treated group. The most potent *Nnmt* ASO (GAAATGAACCAGCAGGCCTT) was chosen for subsequent studies. A control ASO (ISIS 425851), which has no complementarity to any known gene sequence, was used for the control group. *Nnmt* and control ASOs have a uniform phosphorothioate backbone and a

20-base chimaeric design with a 2′-O-(methoxy)-ethyl (2′-MOE) modification on the first five and the last five bases. This modification enhances their binding affinity to complementary sequences and their resistance to the action of nucleases. ASOs may down regulate their target genes through an RNase H-dependent cleavage mechanism or a non-RNA-degrading mechanism by blocking translation of mRNA. Two pathways may be involved ASO entry into cells: first, a productive pathway using a vesicular transport system; and second, a non-productive pathway that results in accumulation of ASOs in lysosomal structures[19].

CLAMS

Energy expenditure was evaluated using a Comprehensive Lab Animal Monitoring System (Columbia Instruments)[33]. HFD-fed mice were treated with *Nnmt*- or control-ASO for 3 weeks. Body weights were not significantly different when the mice were subjected to CLAMS study. The mice were acclimated in the metabolic chambers for 2 days before the experiments. CO_2 and O_2 levels were collected every 32 min for each mouse during a period of 3 days. Food intake and activity were measured at regular intervals.

RNA extraction and quantitative PCR

RNA extraction and Taqman quantitative PCR were performed as described previously[2]. All Taqman primers were purchased from Applied Biosytems, except for the probe for adenosylmethionine decarboxylase (*Amd1*), which was designed using IDT software: forward 5′-GAG AGTGGAATTCGTGACCTG-3′; probe 5′-ACTGTTCAATCCTTGTGGCTAC TCGATG-3′; reverse 5′-TTCTGGTTCTGGAGTGATGTG-3′.

Western blot analysis and immunoprecipitation

NNMT was detected using a chicken anti-NNMT antibody from GenWay Biotech or the rabbit anti-NNMT antibody kindly provided by R. Weinshilboum[34]. Goat anti-UCP1 (M-17) and rabbit anti-PGC1α (H-300) were from Santa Cruz Biotechnology. Rabbit anti-acetylated lysine was from Cell Signaling Technology. For detecting PGC-1α acetylation, PGC-1α was immunoprecipitated from liver or cultured-cell lysates with anti-PGC-1α. The precipitated protein was subjected to western blot analysis using anti-acetylated lysine.

Body composition, body temperature, and faecal lipid excretion

Body composition was analysed in mice treated with *Nnmt* and control ASO for 5 weeks using an EchoMRI 3-in-1 instrument (Echo Medical Systems). To measure body composition after fasting, food was removed from *Nnmt*-ASO- or control-ASO-treated mice for 16h. Body temperature was measured intrarectally using a Thermalert TH-5 thermometer (Physitemp). To analyse faecal lipid excretion, lipid content of faeces was extracted using chloroform:methanol (2:1) and air-dried under a fume hood.

Histology and determination of cell size

Tissues were fixed in 10% buffered formalin and subjected to H&E staining. To measure adipocyte cross-sectional area, four fields of vision of H&E-stained adipose tissue were

digitally photographed under a microscope. Images were analysed using the software ImageJ (National Institutes of Health) using a previously published technique[35]. Images were converted to 16-bit grayscale and inverted; a threshold was applied to identify cell boundaries, and the cells were analysed with the 'Analyze Particles' command to obtain adipocyte area. Adipocyte volume was calculated from the radius using the formula $v = 4/3\pi r^3$.

Intraperitoneal glucose tolerance test

The food was removed from mice for 5 h. Intraperitoneal glucose tolerance test (IPGTT) was performed by intraperitoneal injection of 1 mg glucose per g of body weight. Glucose levels were measured at the indicated times.

Feed efficiency

Total calorie intake was computed from the measured food intake during the second and third weeks of ASO treatment. Feed efficiency was expressed as the body weight gain divided by the total calorie intake between the start and the end of the food intake measurement[36].

Urinary diacetylspermine measurement

Spot urine was collected from *Nnmt*-ASO-and control-ASO-treated mice. Urinary diacetylspermine levels were measured using an ELISA kit from Abnova. An enzymatic mouse creatinine assay (Crystal Chem) was used for measuring creatinine levels. Because the mice drank water ad libitum, the urinary diacetylspermine levels were corrected by creatinine levels. Urinary creatinine levels were not different between *Nnmt*-ASO- and control-ASO-treated mice.

ODC and SSAT activity

ODC and SSAT activities were assayed from tissue supernatant fractions under initial rate conditions with non-limiting substrate concentrations as described previously[37,38]. In brief, ODC was assayed by measuring the release of $^{14}CO_2$ in a reaction with DL-[1-^{14}C]ornithine as the substrate. SSAT was assayed by measuring the formation of acetylated spermidine in a reaction with ^{14}C-CoA and spermidine as co-substrates.

NAD^+ measurement

NAD^+ levels were determined according to instructions provided with the NAD/NADH assay kit purchased from Abcam.

Histone methylation and ChIP-qPCR

Histone protein was extracted from adipose tissue treated with *Nnmt* ASO and control ASO using the EpiQuik Total Histone Extraction Kit from Epigentek. Eight types of histone methylation were measured by western blot analysis using the following antibodies: H3K4me2, H3K9me2, H3K27me2, H3K36me2 and H3K79me2 from Cell Signaling; and H3K4me1, H3K4me3 and H3K9me3 from Abcam. The levels of histone methylation were normalized to total H3 expression. For ChIP, chromatin was first extracted from 3T3-L1

adipocytes treated with or without 10 mM *N*-methylnicotinamide for 48 h. Immunoprecipitation was performed using EpiQuik Methyl-Histone H3-K4 ChIP kit from Epigentek. Enrichment of methylated H3K4 on *Odc* and *Ssat* genes was measured by real-time PCR using EpiTect ChIP qPCR primers from Qiagen (*Odc*, GPM1030188(+)01A; *Ssat*, GPM1055920(+)01A). An open reading frame free region (*Igx1a*) was used as a negative control for ChIP-qPCR. Control IgG showed minimum background among all the regions analysed.

Targeted mass spectrometry

Metabolites nicotinamide, *S*-adenosylmethionine (SAM), *S*-adenosylhomocysteine (SAH), AMP and ATP were measured using tandem mass spectrometry[30,39]. Metabolite extracts using 80% methanol (−80 °C) were dried by nitrogen. Samples were re-suspended using 20 μl LC/MS grade water, of which 10 μl were injected and analysed using a 5500 QTRAP triple quadrupole mass spectrometer (AB/Sciex) coupled to a Prominence HPLC system (Shimadzu) via selected reaction monitoring (SRM). The dwell time was 4 ms per SRM transition and the total cycle time was 1.89 s. Approximately 8 to 11 data points were acquired per detected metabolite. Samples were delivered to the MS using a 4.6 mm internal diameter × 10 cm Amide XBridge HILIC column (Waters) at 300 μl min^{-1}. Gradients were run starting from 85% buffer B (HPLC grade acetonitrile) to 35% B from 0 to 3.5 min; 35% B to 2% B from 3.5 to 11.5 min; 2% B was held from 11.5 to 16.5 min; 2% B to 85% B from 16.5 to 17.5 min; 85% B was held for 7 min to re-equilibrate the column. Buffer A consisted of 20 mM ammonium hydroxide and 20 mM ammonium acetate (pH 9.0) in 95:5 water:acetonitrile. Peak areas from the total ion current for each metabolite SRM transition were integrated using MultiQuant v2.0 software (AB/Sciex).

Cell culture

3T3-L1 cells were differentiated to adipocytes using a standardized protocol[40]. Five to six days after differentiation, cells were transfected using Amaxa electroporation[41]. Hepatoma H2.35 cells were transduced with NNMT or β-galacto-sidase adenovirus for 24 h, and oxygen consumption was measured as described below.

Oxygen consumption

Oxygen consumption was measured with a Clark-type oxygen electrode (Rank Brothers). Cultured cells were trypsinized, counted in a hemocytometer, spun down, and resuspended in respiration buffer (PBS, 2% BSA, 4.5 g l-1 glucose, 120 mg l^{-1} sodium pyruvate) to 1 × 10^6 ml^{-1}. Partial oxygen pressure was recorded using a Rank Brothers digital model 10 controller and a PowerLab 4/30 data acquisition system (ADInstruments)[42].

Statistical test

All data are expressed as mean mean ±s.e.m. Two-tailed Student's *t*-tests were used for single comparisons. Analyses of variance were performed followed by Bonferroni-Holm post-hoc tests for multiple comparisons. Statistical significance is assumed at $P < 0.05$. Sample size was chosen based on results from pilot studies and our extensive experience in investigating metabolic physiology in mice. The sample exclusion criteria were determined

before experiments for technical failures such as mis-injection of glucose in glucose tolerance test. For randomization, experimental groups of mice were stratified according to body weight using an algorithm based on Kullback–Leibler divergences[43]. The CLAMS study, metabolic analyses and oxygen consumption in adipocytes were carried out in a blinded fashion, others were not.

Supplementary Material

Refer to Web version on PubMed Central for supplementary material.

Acknowledgments

We thank R. Weinshilboum for NNMT antibody; P. Woster for DFMO; M. Yuanfor tandem mass spectrometry; A. Karppinen, A. Korhonen, T.Reponen, A. Uimari, S. Pirnes-Karhuand T. Koponen for measurements of ODC and SSAT activity; C. Semenkovich and S. Fried for protocols for FAS activity measurements; and P. Aryal for assistance with real-time qPCR. D.Kr. is supported by the Deutsche Forschungsgemeinschaft (KR 3475/1-1) and American Heart Association (AHA) (09POST2250499); Q.Y. is a Klarman Scholar at the Beth Israel Deaconess Medical Center. This work is supported by grants from the NIH (R37 DK43051, P30 DK57521) and a grant from the JPB foundation to B.B.K.; grants from the NIH (KO8 DK090149, R01 DK100385, BNORC P30 DK046200 and NORCH P30 DK040561) to Q.Y.; grant RO1 DK69966 to P.P.; P01CA120964 and P30CA006516-46 to J.M.A.; AHA 13SDG14620005 and P&F P30 DK0460200 to D.K.; the Ellison Medical Foundation New Scholar in Aging Award to A.A.S.; and academy of Finland grant 118590 to L.A.

References

1. Shepherd PR, Kahn BB. Glucose transporters and insulin action—implications for insulin resistance and diabetes mellitus. N Engl J Med. 1999; 341:248–257. [PubMed: 10413738]
2. Yang Q, et al. Serum retinol binding protein 4 contributes to insulin resistance in obesity and type 2 diabetes. Nature. 2005; 436:356–362. [PubMed: 16034410]
3. Aksoy S, Szumlanski CL, Weinshilboum RM. Human liver nicotinamide *N*-methyltransferase. cDNA cloning, expression, and biochemical characterization. J Biol Chem. 1994; 269:14835–14840. [PubMed: 8182091]
4. Riederer M, Erwa W, Zimmermann R, Frank S, Zechner R. Adipose tissue as a source of nicotinamide *N*-methyltransferase and homocysteine. Atherosclerosis. 2009; 204:412–417. [PubMed: 18996527]
5. Houtkooper RH, Canto C, Wanders RJ, Auwerx J. The secret life of NAD^+: an old metabolite controlling new metabolic signaling pathways. Endocr Rev. 2010; 31:194–223. [PubMed: 20007326]
6. Teperino R, Schoonjans K, Auwerx J. Histone methyl transferases and demethylases; can they link metabolism and transcription? Cell Metab. 2010; 12:321–327. [PubMed: 20889125]
7. Jell J, et al. Genetically altered expression of spermidine/spermine N1-acetyltransferase affects fat metabolism in mice via acetyl-CoA. J Biol Chem. 2007; 282:8404–8413. [PubMed: 17189273]
8. Pirinen E, et al. Enhanced polyamine catabolism alters homeostatic control of white adipose tissue mass, energy expenditure, and glucose metabolism. Mol Cell Biol. 2007; 27:4953–4967. [PubMed: 17485446]
9. Sartini D, et al. Nicotinamide *N*-methyltransferase in non-small cell lung cancer: promising results for targeted anti-cancer therapy. Cell Biochem Biophys. 2013; 67:865–873. [PubMed: 23532607]
10. Ulanovskaya OA, Zuhl AM, Cravatt BF. NNMT promotes epigenetic remodeling in cancer by creating a metabolic methylation sink. Nature Chem Biol. 2013; 9:300–306. [PubMed: 23455543]
11. Williams AC, Cartwright LS, Ramsden DB. Parkinson's disease: the first common neurological disease due to auto-intoxication? QJM. 2005; 98:215–226. [PubMed: 15728403]
12. Lee YH, et al. Microarray profiling of isolated abdominal subcutaneous adipocytes from obese vs non-obese Pima Indians: increased expression of inflammation-related genes. Diabetologia. 2005; 48:1776–1783. [PubMed: 16059715]

13. Salek RM, et al. A metabolomic comparison of urinary changes in type 2 diabetes in mouse, rat, and human. Physiol Genomics. 2007; 29:99–108. [PubMed: 17190852]
14. Yaguchi H, Togawa K, Moritani M, Itakura M. Identification of candidate genes in the type 2 diabetes modifier locus using expression QTL. Genomics. 2005; 85:591–599. [PubMed: 15820311]
15. Wu C, et al. BioGPS: an extensible and customizable portal for querying and organizing gene annotation resources. Genome Biol. 2009; 10:R130. [PubMed: 19919682]
16. Alexander J, Chang GQ, Dourmashkin JT, Leibowitz SF. Distinct phenotypes of obesity-prone AKR/J, DBA2J and C57BL/6J mice compared to control strains. Int J Obes (Lond). 2006; 30:50–59. [PubMed: 16231032]
17. Svenson KL, et al. Multiple trait measurements in 43 inbred mouse strains capture the phenotypic diversity characteristic of human populations. J Appl Physiol. 2007; 102:2369–2378. [PubMed: 17317875]
18. Grubb SC, Maddatu TP, Bult CJ, Bogue MA. Mouse phenome database. Nucleic Acids Res. 2009; 37:D720–D730. [PubMed: 18987003]
19. Bennett CF, Swayze EE. RNA targeting therapeutics: molecular mechanisms of antisense oligonucleotides as a therapeutic platform. Annu Rev Pharmacol Toxicol. 2010; 50:259–293. [PubMed: 20055705]
20. Erion DM, et al. SirT1 knockdown in liver decreases basal hepatic glucose production and increases hepatic insulin responsiveness in diabetic rats. Proc Natl Acad Sci USA. 2009; 106:11288–11293. [PubMed: 19549853]
21. Kang-Lee YA, et al. Metabolic effects of nicotinamide administration in rats. J Nutr. 1983; 113:215–221. [PubMed: 6218261]
22. Varela-Rey M, et al. Fatty liver and fibrosis in glycine *N*-methyltransferase knockout mice is prevented by nicotinamide. Hepatology. 2010; 52:105–114. [PubMed: 20578266]
23. Pegg AE, Casero RA Jr. Current status of the polyamine research field. Methods Mol Biol. 2011; 720:3–35. [PubMed: 21318864]
24. Koponen T, et al. The activation of hepatic and muscle polyamine catabolism improves glucose homeostasis. Amino Acids. 2011; 42:427–440. [PubMed: 21814795]
25. Alcendor RR, et al. Sirt1 regulates aging and resistance to oxidative stress in the heart. Circ Res. 2007; 100:1512–1521. [PubMed: 17446436]
26. Finley LW, et al. Succinate dehydrogenase is a direct target of sirtuin 3 deacetylase activity. PLoS ONE. 2011; 6:e23295. [PubMed: 21858060]
27. Kobayashi Y, et al. SIRT1 is critical regulator of FOXO-mediated transcription in response to oxidative stress. Int J Mol Med. 2005; 16:237–243. [PubMed: 16012755]
28. Stein S, et al. SIRT1 decreases Lox-1-mediated foam cell formation in atherogenesis. Eur Heart J. 2010; 31:2301–2309. [PubMed: 20418343]
29. Rodgers JT, et al. Nutrient control of glucose homeostasis through a complex of PGC-1α and SIRT1. Nature. 2005; 434:113–118. [PubMed: 15744310]
30. Shyh-Chang N, et al. Influence of threonine metabolism on *S*-adenosylmethionine and histone methylation. Science. 2013; 339:222–226. [PubMed: 23118012]
31. Abel ED, et al. Adipose-selective targeting of the *GLUT4* gene impairs insulin action in muscle and liver. Nature. 2001; 409:729–733. [PubMed: 11217863]
32. Shepherd PR, et al. Adipose cell hyperplasia and enhanced glucose disposal in transgenic mice overexpressing GLUT4 selectively in adipose tissue. J Biol Chem. 1993; 268:22243–22246. [PubMed: 8226728]
33. Bubolz AH, et al. Activation of endothelial TRPV4 channels mediates flow-induced dilation in human coronary arterioles: role of Ca^{2+} entry and mitochondrial ROS signaling. Am J Physiol Heart Circ Physiol. 2012; 302:H634–H642. [PubMed: 22140047]
34. Yan L, Otterness DM, Craddock TL, Weinshilboum RM. Mouse liver nicotinamide *N*-methyltransferase: cDNA cloning, expression, and nucleotide sequence polymorphisms. Biochem Pharmacol. 1997; 54:1139–1149. [PubMed: 9464457]

35. Chen HC, Farese RV Jr. Determination of adipocyte size by computer image analysis. J Lipid Res. 2002; 43:986–989. [PubMed: 12032175]
36. Bence KK, et al. Neuronal PTP1B regulates body weight, adiposity and leptin action. Nature Med. 2006; 12:917–924. [PubMed: 16845389]
37. Bernacki RJ, et al. Preclinical antitumor efficacy of the polyamine analogue N1, N11-diethylnorspermine administered by multiple injection or continuous infusion. Clin Cancer Res. 1995; 1:847–857. [PubMed: 9816054]
38. Jänne J, Williams-Ashman HG. On the purification of L-ornithine decarboxylase from rat prostate and effects of thiol compounds on the enzyme. J Biol Chem. 1971; 246:1725–1732. [PubMed: 5547701]
39. Yang X, et al. Using tandem mass spectrometry in targeted mode to identify activators of class IA PI3K in cancer. Cancer Res. 2011; 71:5965–5975. [PubMed: 21775521]
40. Yan QW, et al. The adipokine lipocalin 2 is regulated by obesity and promotes insulin resistance. Diabetes. 2007; 56:2533–2540. [PubMed: 17639021]
41. Eguchi J, et al. Interferon regulatory factors are transcriptional regulators of adipogenesis. Cell Metab. 2008; 7:86–94. [PubMed: 18177728]
42. Pulinilkunnil T, et al. Adrenergic regulation of AMP-activated protein kinase in brown adipose tissue *in vivo*. J Biol Chem. 2011; 286:8798–8809. [PubMed: 21209093]
43. Endo A, Nagatani F, Hamada C, Yoshimura I. Minimization method for balancing continuous prognostic variables between treatment and control groups using Kullback–Leibler divergence. Contemp Clin Trials. 2006; 27:420–431. [PubMed: 16807130]

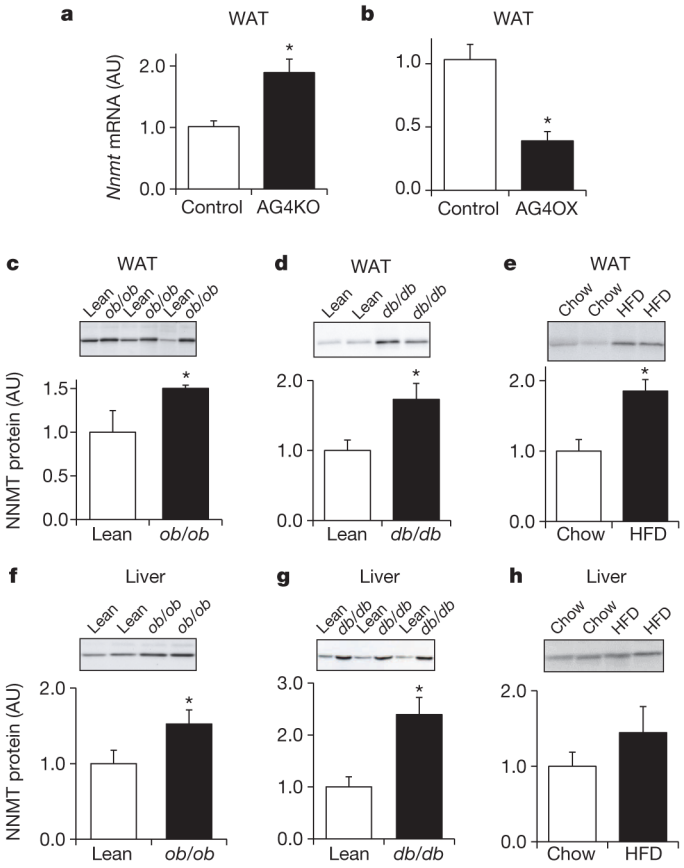

Figure 1. NNMT expression is increased in WAT and liver of obese and insulin-resistant mice

a, **b**, *Nnmt* mRNA expression normalized by cyclophilin in WAT of adipose-specific *Glut4* knockout (AG4KO) mice and aP2-Cre controls (*n* =4 per group) (**a**) and adipose-specific *Glut4* overexpressing (AG4OX) and wild-type littermate controls (*n* =6 per group) (**b**). **c–e**, NNMT protein levels in WAT of *ob*/*ob* mice (*n* =8) and lean controls (*n* =4) (**c**); *db*/*db* mice and lean controls (*n* =7 per group) (**d**), and high-fat diet (HFD)-fed (*n* =6) and chow-fed mice (*n* =7) (**e**). **f–h**, NNMT protein levels in liver of *ob*/*ob* mice (*n* =9) and lean controls (*n* =6) (**f**); *db*/*db* mice and lean controls (*n* =7 per group) (**g**); and HFD-fed and chow-fed mice (*n* =6 per group) (**h**). Actin was used as a control for western blot analysis and the levels were not different between lean and obese mice. AU, arbitrary units. Error bars, ±s.e.m; **P* <0.05.

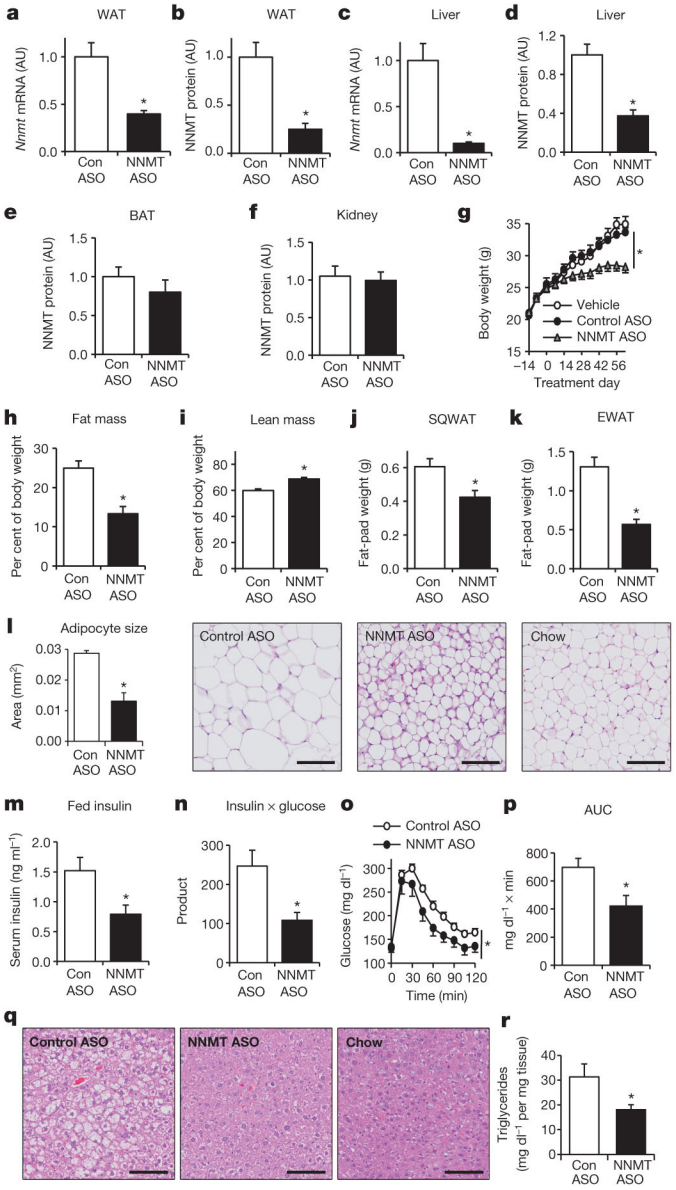

Figure 2. *Nnmt* knockdown prevents diet-induced obesity and insulin resistance

a–f, Knockdown efficiency of *Nnmt*-ASO. mRNA expression was normalized by cyclophilin and protein levels were corrected with actin levels: *Nnmt* mRNA (**a**) and NNMT protein in WAT (**b**); *Nnmt* mRNA (**c**) and NNMT protein in liver (**d**); NNMT protein in brown adipose tissue (BAT) (**e**) and kidney (**f**). **g**, Body weights of C57BL/6 mice fed a high-fat diet and treated with *Nnmt* ASO, control ASO, or vehicle (saline) for 8 weeks. **h**, Fat mass as a percentage of body weight. **i**, Lean mass as a percentage of body weight. **j**, Subcutaneous WAT (SQWAT) fat-pad weights. **k**, Epididymal WAT (EWAT) fat-pad weights. **l**, Epididymal adipocyte cross-sectional area and haematoxylin and eosin (H&E)-stained sections of SQWAT. **m**, Serum insulin levels. **n**, Glucose × insulin product (ng ml^{-1} × mg dl^{-1}) in the fed state. **o**, Intraperitoneal glucose tolerance test. **p**, Area under the curve (AUC) of the glucose tolerance. **q**, H&E stain of liver sections of HFD-fed *Nnmt*-ASO-and

control-ASO-treated mice, and of chow-fed mice. **r**, Hepatic triglyceride levels in *Nnmt*- and control-ASO-treated mice. The scale bars in **l** and **q** represent 100 μm; *n* =8 per group for **a**–**p**, *n* =13 per group for **r**. AU, arbitrary units. Error bars, ±s.e.m.; **P* <0.05.

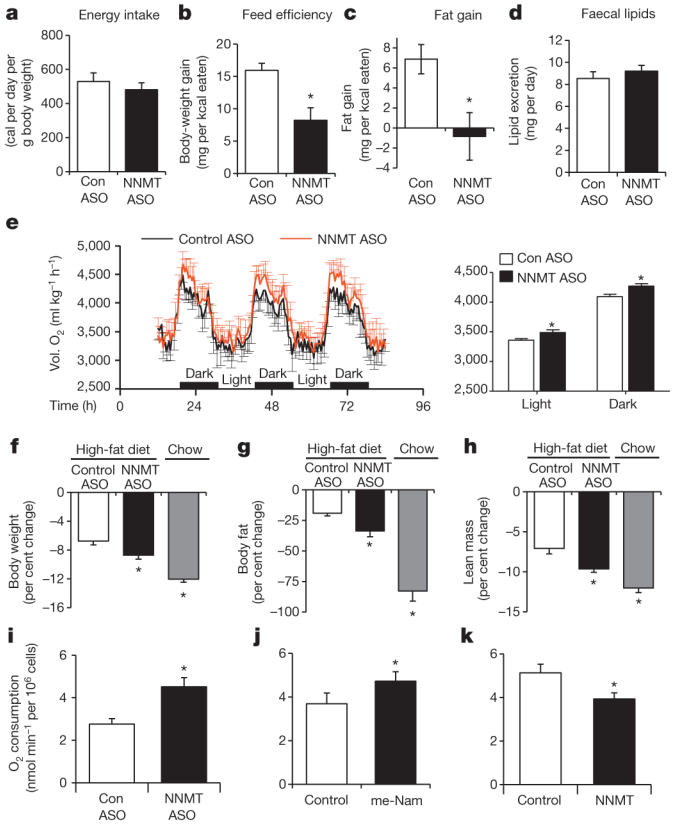

Figure 3. NNMT regulates energy expenditure

a, Energy intake of HFD-fed control-ASO- and *Nnmt*-ASO-treated mice. **b**, Feed efficiency (body-weight gain per kilocalorie (kcal) consumed) of HFD-fed control-ASO- and *Nnmt*–ASO-treated mice. **c**, Fat mass gain per kcal consumed in HFD-fed mice treated with *Nnmt* ASO or control ASO. *n* =12 per group for **a**–**c. d**, Faecal lipid excretion (*n* =10 per group). **e**, Oxygen consumption (Vol. O_2) measured by CLAMS (*n* =7 per group). **f–h**, Effects of a 16-h fast on body weight (**f**), fat mass (**g**), and lean body mass (*n* =8 per group) (**h**). **i–k**, Oxygen consumption in 3T3-L1 adipocytes transfected with control or *Nnmt* ASO (*n* =6 per group) (**i**), treated with 10 mM N^1-methylnicotinamide (me-Nam) (*n* =6 per group) (**j**), or transfected with *Nnmt* cDNA (*n* =10 per group) (**k**). Error bars, ±s.e.m.; **P* <0.05.

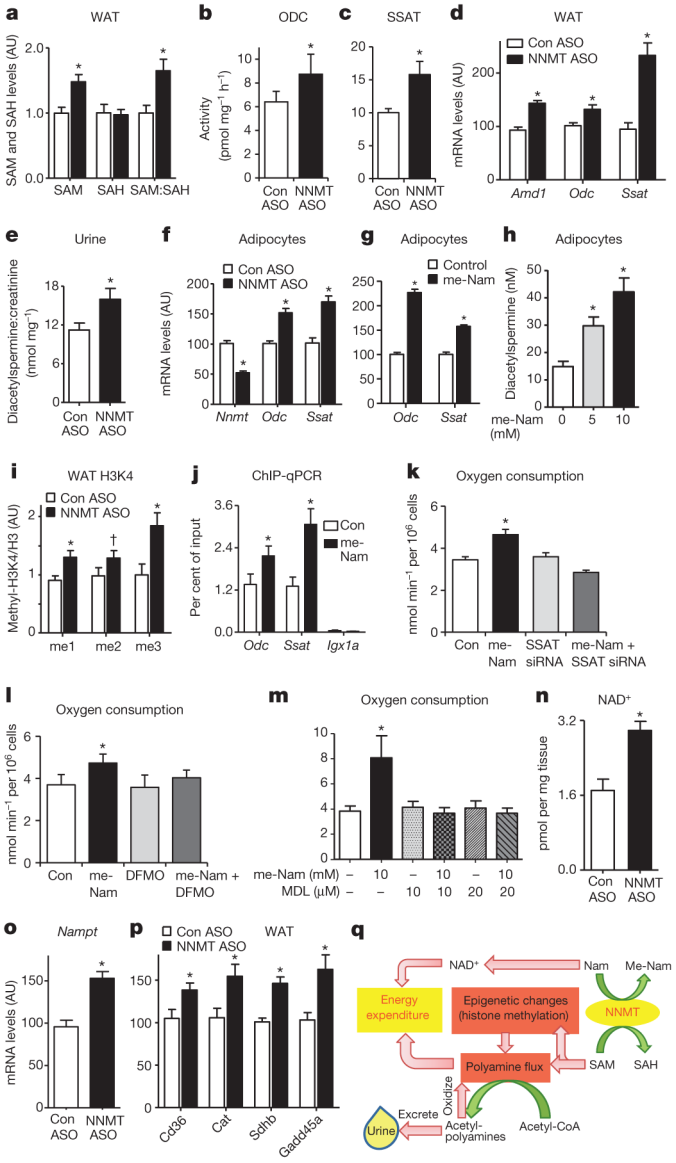

Figure 4. NNMT regulates SAM and NAD$^+$ pathways in adipose tissue

a, Adipose *S*-adenosylmethionine (SAM), *S*-adenosylhomocysteine (SAH) and SAM:SAH ratio measured by LC–MS/MS (*n* =8 for control-ASO-treated mice; *n* =12 for *Nnmt*-ASO-treated mice). **b**, **c**, ODC (**b**) and SSAT (**c**) activity (*n* =10 per group). **d**, *Amd1*, *Odc* and *Ssat* mRNA expression in adipose tissue of *Nnmt*-ASO- and control-ASO-treated mice (*n* =12 per group). **e**, Urinary diacetylspermine:creatinine ratio (*n* =22 for control-ASO-treated mice; *n* =29 for *Nnmt*-ASO-treated mice). **f**, **g**, *Odc* and *Ssat* mRNA levels in 3T3-L1 adipocytes with *Nnmt* knockdown (*n* =9 per group) (**f**) and N^1-methylnicotinamide (me-Nam) (**g**) treatment (*n* =6 per group). **h**, Diacetylspermine secretion from 3T3-L1 adipocytes treated with me-Nam (*n* =10 per group). **i**, Expression of mono-, di- and tri-methylation of lysine histone 3 (H3K4) normalized to total H3 levels in adipose tissue (*n* =8 per group). **j**, H3K4me2 occupancy on *Odc*, *Ssat* genes and an open reading frame free region (*Igx1a*) as a negative control in adipocytes measured by ChIP-qPCR (*n* =12 per group). **k–m**, Oxygen

consumption in adipocytes transfected with control or *Ssat* siRNA, and treated with or without 10 mM me-Nam (n =6 per group) (**k**); treated with 10 mM me-Nam with or without 5 mM difluoromethylornithine (DFMO), a specific ODC inhibitor (n =6 per group) (**l**); or treated with 10 mM me-Nam with or without MDL72527, a specific PAO inhibitor (n =6 per group) (**m**). **n**, NAD^+ levels (n =7 Con-ASO; n =12 *Nnmt* ASO). **o**, mRNA levels of nicotinamide phosphoribosyltransferase (*Nampt*) (n =11 per group). **p**, mRNA levels of SIRT1 target genes: *Cd36*, catalase (*Cat*), succinate dehydrogenase B (*SdhB*) and growth arrest and DNA-damage-inducible protein (*Gadd45a*) in adipose tissue of NNMT-ASO- and control-ASO treated mice (n =11 per group). Error bars, ± s.e.m., *P <0.05, †P =0.06. **q**, Model of NNMT-regulated energy expenditure in adipocytes. NNMT methylates nicotinamide (Nam), a precursor of NAD^+, using SAM as a methyl donor. SAM regulates polyamine flux by providing substrates and modulating histone methylation. Polyamine flux utilizes acetyl-CoA to generate acetyl-polyamines, which are oxidized or excreted in the urine. Taken together, this results in adipose metabolic substrate consumption and loss coupled with systemic alteration of energy expenditure.